Prolonged nicotine exposure reduces aversion to the drug in mice by altering nicotinic transmission in the interpeduncular nucleus.

Sarah Mondoloni[1], Claire Nguyen[1], Eléonore Vicq[1,2], Joachim Jehl[1,2], Romain Durand-de Cuttoli[1], Nicolas Torquet[1], Stefania Tolu[1], Stéphanie Pons[3], Uwe Maskos[3], Fabio Marti[1,2], Philippe Faure[1,2*] and Alexandre Mourot[1,2*]

Affiliations:

1. Sorbonne Université, Inserm, CNRS, Neuroscience Paris Seine - Institut de Biologie Paris Seine (NPS - IBPS), 75005 Paris, France.

2. Brain Plasticity Unit, CNRS, ESPCI Paris, PSL Research University, 75005 Paris, France

3. Institut Pasteur, Unité Neurobiologie intégrative des systèmes cholinergiques, Département de neuroscience, 75724 Paris cedex, France.

* equal contributions

Correspondence to: almourot@gmail.com or phfaure@gmail.com

Keywords: nicotinic acetylcholine receptors, nicotine addiction, two-bottle choice paradigm, drug aversion, medial habenula-interpeduncular nucleus pathway

Abstract

Nicotine intake is likely to result from a balance between the rewarding and aversive properties of the drug, yet the individual differences in neural activity that control aversion to nicotine and their adaptation during the addiction process remain largely unknown. Using a two-bottle choice experiment, we observed a high heterogeneity in nicotine-drinking profiles in isogenic adult male mice, with about half of the mice persisting in consuming nicotine even at high concentrations, whereas the other half durably stopped consumption. We found that nicotine intake was negatively correlated with nicotine-evoked currents in the interpeduncular nucleus (IPN), and that prolonged exposure to nicotine, by weakening this response, decreased aversion to the drug, and hence boosted consumption. Lastly, using knock-out mice and local gene re-expression, we causally identified β4-containing nicotinic acetylcholine receptors of IPN neurons as the molecular and cellular correlates of nicotine aversion. Collectively, our results identify the IPN as a substrate of individual variabilities and adaptations in nicotine consumption.

Introduction

Nicotine remains the most-widely used addictive substance in the world, and even though cigarette smoking is overall decreasing, the use of new products such as electronic cigarettes has risen dramatically in recent years [1]. Nicotine administration induces a series of effects, ranging from pleasurable (i.e. appetitive, rewarding, reinforcing, anxiolytic…) to noxious (i.e. anxiogenic, aversive…) [2]. These multifaceted effects have been described both in humans and in rodents[2]. They greatly depend on the dose of nicotine administered, show substantial inter-individual variability, and are believed to be key in the regulation of nicotine intake and in the maintenance of addiction [2,3]. Understanding the variable effects of nicotine at the molecular and circuit levels is therefore fundamental to progress in the pathophysiology of nicotine addiction, and to develop efficient smoking-cessation therapies.

Nicotine mediates its physiological effects by activating nicotinic acetylcholine receptors (nAChRs), pentameric ligand-gated ion channels encoded by a large multigene family. There are nine nAChR α (α2-10) and three β (β2-4) subunits expressed in the brain, which can assemble to form homo-pentamers or hetero-pentamers with various localizations and functions [4,5]. Initiation of consumption and reinforcement to nicotine involve the mesolimbic dopamine reward circuit, which originates in the ventral tegmental area (VTA) [6]. Nicotine primarily acts on this circuit by activating α4β2 nAChRs, a receptor subtype that displays high affinity for the drug [6-9]. Interestingly, an acute injection of nicotine also inhibits a subset of VTA dopamine neurons that project to the amygdala [10], and this results in elevated anxiety in mice,

illustrating the heterogeneity of the brain reward circuit, and the complexity of nicotine dependence.

Another important pathway in the neurobiology of nicotine addiction is the medial habenulo-interpeduncular (MHb-IPN) axis [11-14]. This pathway is deeply implicated in the regulation of aversive physiological states such as fear and anxiety [15-17]. It is believed to directly mediate aversion to high doses of nicotine [11,12], to trigger the affective (anxiety) and somatic symptoms following nicotine withdrawal [18-21] and to be involved in relapse to nicotine-seeking [22]. Strikingly, neurons of the MHb-IPN axis express the highest density and largest diversity of nAChRs in the brain, notably the rare α5, α3 and β4 subunits [5]. These are encoded by the CHRNA5-A3-B4 gene cluster, of which some sequence variants are associated with a high risk of addiction in humans [23,24]. The α3 and β4 subunits are virtually absent in the VTA, or in other parts of the brain. The α3β4 nAChR shows lower affinity for nicotine than the α4β2 subtype, which has contributed to the widely accepted idea that nicotine is rewarding at low doses because it activates primarily α4β2 receptors of the VTA, while it is aversive at high doses because only then does it activate α3β4 nAChRs of the MHb-IPN axis [11,13]. Nevertheless, this hypothesis of different reactivity thresholds to nicotine in different circuits is based on indirect evidence from c-fos quantification or brain slice physiology experiments, and does not take into account the possible adaptive changes in the circuits that result from repeated exposure to nicotine. Therefore, real-time recording of the response of the MHb-IPN circuit to nicotine, both in naive animals and after prolonged exposure to nicotine, is still a prerequisite to understand the mechanism by which smokers develop tolerance to the aversive effects of nicotine.

88 A distinct feature of addiction is that, overall, only some individuals lose control over
89 their drug use, progressively shifting to compulsive drug intake [25-29]. About a third to
90 half of those who have tried smoking tobacco become regular users [30]. Individual
91 differences in the sensitivities of the VTA and MHb-IPN systems, and in their respective
92 adaptations during chronic tobacco use, could contribute to the vulnerability to nicotine
93 and to the severity of the addiction process [13,31-34]. Yet, the neural mechanism that
94 makes individuals more prone to maintain nicotine consumption versus durably stop
95 are unclear. In addition, whether the MHb-IPN pathway respond differently to nicotine
96 in individuals with and without a history of nicotine use is largely unknown. Here we
97 used isogenic mice and electrophysiology (*ex vivo* and *in vivo*) to study the neuronal
98 correlates of inter-individual variabilities in nicotine consumption behavior, and their
99 adaptation after chronic exposure to the drug.
100
101
102 **Results**
103
104 <u>Heterogeneity in nicotine consumption in isogenic wild-type mice.</u>
105
106 We used a continuous access, two-bottle choice nicotine-drinking test to assess
107 consumption profiles in wild-type C57Bl6 male mice single-housed in their home cage
108 (Fig. 1A). In this test, animals have continuous and concurrent access to two bottles
109 containing a solution of either 2% saccharine (vehicle) or nicotine plus 2% saccharine
110 (to mask the bitter taste of nicotine). After a 4-day habituation period with water in both
111 bottles, nicotine concentration was progressively increased in one bottle across 16
112 days, from 10 to 200 μg/ml (4 days at each concentration), while alternating the side

113 of the nicotine-containing solution every other day to control for side bias (Fig. 1B).
114 Consumption from each bottle was measured every minute. We found that the daily
115 nicotine dose consumed increased throughout the paradigm, to stabilize at about 10
116 mg/kg/day on average for the highest nicotine concentration tested (Fig. 1C, Fig. S1A).
117 The progressive increase in nicotine consumption was associated with an overall
118 decrease in the preference for nicotine, especially for concentrations above 50 μg/ml
119 (Fig. 1D). At the population level, these results suggest that mice adjust their daily dose
120 of nicotine by selecting the adapted bottle according to their own preference for the
121 drug, resulting in nicotine titration, as previously reported [11,33].
122
123 We then analyzed more precisely individual nicotine consumption profiles, and found
124 two major types of behaviors. About half of the mice (18/35) displayed a gradual
125 increase or reached a particular plateau in their consumption, and still had significant
126 consumption for the highest dose tested. We classified these mice as "consumers"
127 (Fig. 1E). The other half of the mice (17/35) unexpectedly avoided the nicotine-
128 containing bottle, either right at the beginning of the task, or at the transition to specific
129 nicotine doses during the task. We classified these mice as "avoiders". Overall, only
130 a small proportion of the mice (7/35) readily titrated their nicotine intake, which
131 contrasts with what can be observed at the population level here (Fig. 1C) and in
132 previous studies [11,33]. Avoiders and consumers (defined as above throughout the
133 manuscript) showed on average similar nicotine intake for the low concentrations of
134 nicotine (10 and 50 μg/ml, $p > 0.05$), but while nicotine intake increased throughout the
135 task for consumers (16.9 ± 2.9 mg/kg/day for 200 μg/ml of nicotine) it dropped down
136 to 2.6 ± 0.4 mg/kg/day for such high nicotine concentration in avoiders (Fig. 1F), and
137 almost reached zero over the last three days (Fig. 1G). The preference ratio in

138 consumers was fairly constant throughout the task (Fig. S1B), whereas in avoiders,
139 preference for nicotine drastically decreased as nicotine concentration increased (Fig.
140 S1B), with a pattern similar to what we observed in a two-bottle choice quinine-drinking
141 test (Fig. S1C), suggesting that avoiders have actually developed aversion to nicotine.
142
143 The dose of nicotine triggering aversion differs between mice
144
145 The average consumption over four days is a good indicator of the drug dose
146 consumed and preference ratio. However, it does not take into account the choice
147 patterns of the animals and their behavioral adaptations when bottles are swapped.
148 Due to the oral nature of the test, it may be difficult for an animal to associate
149 consumption in a particular bottle with the effects (whether positive or negative) of
150 nicotine. We thus systematically analyzed individual preference ratios throughout the
151 task. We found that some consumers actively tracked the side associated with nicotine
152 when bottles were swapped (e.g. mouse #1 in Fig. 2A), indicating preference for the
153 bottle containing nicotine, while others displayed a strong side preference and never
154 alternated drinking side (e.g. mouse #2 in Fig. 2A), and hence consumed nicotine in a
155 more passive fashion. In contrast, all avoider mice (n = 17) readily displayed actual
156 avoidance behavior of the nicotine-containing solution, whether they initially tracked
157 the nicotine solution (e.g. mice #3 and 5 in Fig. 2A) or not (e.g. mice #4 and 6 in Fig.
158 2A). To quantify the evolution of nicotine preference at the individual level throughout
159 the task, and to better take into account the passive consumption behavior of some of
160 the mice, we mapped each profile in a pseudo-ternary plot where two apices represent
161 100% saccharine (Sacc.) and 100% nicotine (Nic.) preference, while the third apex
162 represents 100% side bias (Fig. 2B). Such a ternary representation enabled us to

163 represent the trajectory for each individual, from the water condition to the 200 μg/ml
164 nicotine condition, and to calculate the shortest distance from the point of interest to
165 each apex, at each step of the task. We found that the behavior of consumers was on
166 average fairly consistent throughout the task, i.e. their distance from the apex was not
167 really impacted by the nicotine dose (Fig. 2C and Fig. S2). In contrast, the behavior of
168 avoiders was highly nicotine dose-dependent, with mice going further away from the
169 nicotine apex as nicotine concentration increases (Fig. 2 C and Fig. S2). Aversion to
170 nicotine in avoider mice mainly occurred at the transition from 100 to 200 μg/ml, but
171 some mice displayed a threshold as low as 10 μg/ml for avoidance-like behavior. In
172 fact, the proportion of avoiders progressively developed as nicotine concentration
173 increased in the bottle, to reach about 50% at the end of the 20-day task (Fig. 2D).
174 Together, these results indicate that most mice can discriminate nicotine from the
175 control solution and that, at some specific threshold dose, some mice start actively
176 avoiding the nicotine-containing bottle.
177
178 Do avoiders readily and durably learn to avoid the nicotine-containing solution, or do
179 they just rapidly react to the dose to adjust their intake? To answer this question, we
180 added at the end of the two-bottle choice task, i.e. after the 200 µg/ml nicotine
181 condition, a condition with a low concentration of nicotine (50 µg/ml). We chose 50
182 µg/ml of nicotine because avoiders and consumers initially displayed comparable
183 nicotine intake and preference at this dose (Fig. 1F, Fig. S1B). We hypothesized that
184 if avoiders increased their preference at the 200-50 µg/ml transition, it would indicate
185 a rapid adjustment to the concentration proposed. In contrast, if avoiders maintained
186 a steady, low preference for nicotine, it would indicate that a threshold was reached
187 during previous exposure and that nicotine aversion became persistent, independently

188 of the dose. We found that indeed lowering nicotine concentration from 200 to 50 µg/ml
189 did not increase the nicotine preference ratio in avoiders (Fig. 2E), thus indicating that
190 wild-type (WT) mice can develop learned aversion for nicotine during a self-
191 administration task, which results in a durable change in behavior and nearly-complete
192 cessation of consumption.
193
194 Nicotine consumption negatively correlated with the amplitude of nicotine-evoked
195 currents in the IPN
196
197 We then hypothesized that the IPN, which is involved in nicotine aversion and in
198 negative affective states [2,35,36], might be differently activated by nicotine in avoiders
199 and consumers. We used patch-clamp electrophysiology on brain slices to assess, at
200 completion of the two-bottle choice task, the functional expression level of nAChRs in
201 IPN neurons. We recorded neurons from the dorsal and rostral IPN because these
202 neurons have high nAChR density [13,14,37,38]. To record nicotine-evoked currents, we
203 used a local puff application of nicotine at a concentration (30 µM) close to the EC50
204 for heteromeric nAChRs [39]. We found that the amplitude of nicotine-induced currents
205 was higher in IPN neurons of avoider mice than in consumers (Fig. 2F). Moreover, we
206 found a negative correlation between the average amplitude of nicotine-induced
207 current in IPN neurons, and nicotine consumption levels (measured over the last 24
208 hours prior to the patch-clamp recording, Fig. 2G), suggesting that nicotine
209 consumption level in mice is negatively linked to the amplitude of the response to
210 nicotine in IPN neurons.
211

212 Chronic nicotine treatment alters both nicotinic signaling in the IPN and nicotine
213 consumption.
214
215 It is still unclear at this stage whether chronic nicotine exposure progressively alters
216 the response of IPN neurons to the drug (consumers being further exposed to high
217 nicotine doses than avoiders) or whether an intrinsic difference pre-exists in consumer
218 and avoiders. To determine the effect of chronic nicotine exposure on nAChR current
219 levels in IPN neurons, we passively and continuously exposed mice to nicotine for 4
220 weeks, using subcutaneously implanted osmotic minipumps. The concentration of
221 nicotine in the minipump (10 mg/kg/day) was chosen to match the average voluntary
222 intake of nicotine in the two-bottle choice task (Fig. 1C). We then recorded nicotine-
223 evoked currents from acute brain slices and found that indeed, prolonged exposure to
224 nicotine reduced the amplitude of nicotine-evoked currents in the IPN of these mice
225 compared to control mice treated with saline (Fig. 3A). These results are consistent
226 with the reduced current amplitudes we observed in mice that underwent the two-bottle
227 choice task, compared to naive mice in their home cage (Fig S3A). Because IPN
228 neurons are mostly silent in brain slices, and in order to preserve the entire circuitry
229 intact, we decided to perform juxtacellular recordings of IPN neurons *in vivo*, and to
230 characterize their response (expressed in % of variation from baseline) to an
231 intravenous (i.v.) injection of nicotine (30 µg/kg). To our knowledge, no description of
232 *in vivo* recordings of IPN neurons, and thus no criteria for identification have been
233 reported as yet, hence we solely considered neurons that were labelled *in vivo* with
234 neurobiotin and confirmed to be within the IPN for the analysis. We found that nicotine
235 i.v. injections in naive WT mice induced an increase in the firing rate of IPN neurons
236 compared to an injection of saline, and that this acute effect of nicotine was reduced

237 after the prolonged (4 weeks) passive exposure of mice to the drug (Fig.3B). Some of
238 the IPN neurons, however, responded to nicotine by decreasing their firing rate, and
239 the degree of inhibition was lower in the group exposed to chronic nicotine (Fig. S3B).
240 Together, these *ex vivo* and *in vivo* recordings demonstrate that prolonged exposure
241 to nicotine markedly reduces nicotine-evoked responses in mouse IPN neurons.
242
243 To verify the hypothesis that a modification in the cholinergic activity of IPN neurons
244 impacts nicotine aversion, we first evaluated the consequence of prolonged nicotine
245 exposure on nicotine consumption. Mice were implanted with an osmotic minipump to
246 passively deliver nicotine and, after 20 days, were subjected to a modified two-bottle
247 task that consisted in a rapid presentation to high doses (100 µg/ml) of nicotine (Fig.
248 3C). We chose this protocol to avoid the confounding effects of a gradual exposure to
249 nicotine. We found that mice pretreated with saline (controls), but not those pretreated
250 with nicotine, significantly decreased their preference for the nicotine-containing
251 solution (Fig. 3C), gradually over the four days (Fig. S3C). This indicates that mice
252 under chronic nicotine treatment developed tolerance for the aversive effects of
253 nicotine. Overall, this resulted in greater nicotine intake for the group treated with
254 nicotine than for the group treated with saline (Fig. 3C). When focusing on individuals,
255 we observed that a single saline-pretreated mouse (1/23) increased its nicotine
256 preference when nicotine was introduced in the task, while the great majority of the
257 mice actively avoided nicotine. In contrast, a large proportion of the mice treated with
258 nicotine (8/25) increased their preference for nicotine (Fig.3D). The two groups were
259 identical in the water/water session. However, in the water/nicotine session, mice
260 pretreated with nicotine showed a greater distance from the “Saccharine apex”, and a
261 shorter distance from the “Nicotine apex” than mice pretreated with saline in the

262 pseudo ternary representation (Fig. 3E), indicating increased reference for the drug in
263 the nicotine pretreated group. Altogether, these electrophysiological and behavioral
264 data demonstrate that prolonged exposure to nicotine both decreases nicotine efficacy
265 in the IPN, and also increases the threshold for triggering nicotine-aversion in
266 individuals, resulting in increased consumption of the drug. Yet, whether these
267 electrophysiological and behavioral effects are causally related remains to be
268 demonstrated.
269
270 Nicotine avoidance involves β4*nAChRs.
271
272 We turned to mutant mice deleted for the gene encoding the nAChR β4 subunit ($\beta4^{-/-}$
273 mice), because of the strong and restricted expression of this subunit in the IPN [31,40,41].
274 We found that $\beta4^{-/-}$ mice displayed both greater nicotine preference and greater
275 consumption than WT animals, with virtually no dose-dependent change in nicotine
276 preference (Fig. 4A). When looking at individuals, we observed both active and passive
277 nicotine-drinking profiles in $\beta4^{-/-}$ mice, as already observed in WT mice (13/35 passive
278 mice for WT mice; 4/13 for $\beta4^{-/-}$ mice). Strikingly, none of the $\beta4^{-/-}$ mice (0/13) showed
279 aversion-like behavior at high nicotine doses, which contrasts with the high proportion
280 of avoiders in WT animals (17/35, Fig. 4B, Fig. S4A). WT mice showed a strong
281 adaptation in their behavior according to the dose of nicotine, while $\beta4^{-/-}$ mice had a
282 more consistent behavior throughout the task (Fig. 4C and Fig. S4B, C).
283
284 To verify that responses to nicotine were affected in IPN neurons of $\beta4^{-/-}$ mice, we
285 performed patch-clamp recordings. We found that the amplitude of nicotine-evoked
286 currents in the IPN was on average three-fold lower in $\beta4^{-/-}$ than in WT mice (Fig. 4D),

287 confirming that β4*nAChRs are the major receptor subtype in the IPN. Furthermore,
288 prolonged nicotine treatment had no significant effect on the amplitude of nAChR
289 currents in these knock-out mice (Fig. 4D), suggesting that the downregulation
290 observed after chronic nicotine treatment in the IPN of WT mice mainly affects
291 β4*nAChRs. We then used *in vivo* juxtacellular recordings, and performed dose-
292 response experiments (7.5 – 30 μg/kg) in order to assess the role of β4*nAChRs in the
293 response to different doses of nicotine. In WT mice, nicotine i.v. injections resulted in
294 a dose-dependent increase in IPN neuron activity (Fig. 4E). In $\beta4^{-/-}$ mice, responses to
295 nicotine were of smaller amplitude, especially for the highest dose of nicotine tested
296 (Fig. 4E), further demonstrating the important role of β4*nAChRs of the IPN in the
297 response to nicotine. In both WT and $\beta4^{-/-}$ mice, we observed a population of neurons
298 that decreased their firing rate in a dose-dependent manner, yet with no difference in
299 the amplitude of the response between the two genotypes (Fig. S4D-F), suggesting
300 that β4*nAChR are mainly involved in the increase, but not in the decrease, of neuronal
301 activity in response to nicotine injection. Collectively, our results in $\beta4^{-/-}$ mice
302 demonstrate the key role of the nAChR β4 subunit in signaling aversion to nicotine,
303 and its predominant role in sensing nicotine and activating the IPN.
304
305 <u>β4*nAChRs of the IPN are critically involved in nicotine aversion.</u>
306
307 To causally assess the role of β4*nAChRs of IPN neurons in nicotine aversion, and
308 more generally in nicotine consumption, we targeted re-expression of β4 in the IPN
309 specifically, using lentiviral vectors in $\beta4^{-/-}$ mice (KO-$\beta4^{IPN}$ mice, Fig. 5A). Mice
310 transduced with eGFP (KO-GFP^{IPN} mice) were used as controls. Proper transduction
311 in the IPN was verified using immunohistochemistry after completion of the two-bottle

312 choice task (Fig. 5A), and mice with expression of GFP in the VTA were excluded from
313 analyses. Transduction of β4, but not of GFP, in the IPN increased the amplitude of
314 nicotine-evoked currents (Fig. 5B) and restored levels found in WT animals (U test, p
315 = 0.6, Fig. S5A). We compared nicotine intake in the two groups of mice in the two-
316 bottle choice task. We found that re-expression of β4 in the IPN of $\beta4^{-/-}$ mice decreased
317 nicotine consumption compared to the group of mice transduced with eGFP in the IPN
318 (Fig. 5C). Overall, consumption levels were similar in WT and in KO-$\beta4^{IPN}$ animals
319 ($p>0.5$ for all doses), demonstrating the causal role of β4 nAChRs of IPN neurons in
320 nicotine consumption behaviors. At the individual level, the proportion mice that
321 avoided nicotine at 200 μg/kg was very low (11% avoiders) for KO-GFP^{IPN} control mice,
322 but greater for KO-$\beta4^{IPN}$ mice (47% avoiders, Fig. 5D). The behavior of KO-GFP^{IPN}
323 was steady throughout the task, whereas it was highly nicotine-dose dependent for
324 KO-$\beta4^{IPN}$ mice (Fig. 5E and Fig. S5B, C), as already observed with WT mice. Mice with
325 strong preference for nicotine were only found in the KO-GFP^{IPN} control group.
326 Collectively, these results show that re-expression of β4 in the IPN of $\beta4^{-/-}$ mice rescued
327 aversion for nicotine, and highlight the specific role of β4*nAChRs of IPN neurons in
328 setting the threshold dose for aversion to nicotine, and in the control of nicotine intake.
329

330 **Discussion**

331

332 We used a two-bottle choice paradigm to assess inter-individual differences in nicotine
333 consumption in mice, and to evaluate how pre-exposure to nicotine modifies drug
334 taking. Oral self-administration is a classical method for chronic nicotine administration
335 as it provides rodents with *ad libitum* access to nicotine, likely mimicking administration
336 in human smokers, while minimizing stress from handling [42]. We observed that, on

337 average, WT mice titrate their intake to achieve a consistent nicotine dose, in
338 agreement with previous reports [11,33,34], and discovered that mutant mice lacking the
339 nAChR β4 subunit did not, resulting in greater nicotine consumption, notably at high
340 nicotine concentrations of the drinking solution. These behavioral results are in
341 agreement with the greater intracranial self-administration observed at high nicotine
342 doses in these mice [32] and, conversely, with the results obtained with transgenic
343 TABAC mice overexpressing the β4 subunit at endogenous sites, which avoid nicotine
344 and as a consequence consume very little [12,32]. Nevertheless, it should be noted that
345 conflicting results have also been reported regarding the role of β4 nAChRs in nicotine
346 consumption. Notably, intravenous self-administration of nicotine is lower in $\beta4^{-/-}$ mice
347 despite a higher sensitivity of the VTA to nicotine in these mice [31], and self-
348 administration is higher in TABAC mice despite reduced nicotine-induced activation of
349 the VTA [43]. The increased consumption at high nicotine doses reported here for $\beta4^{-/-}$
350 mice resembles what was observed in mutant mice either lacking the α5 subunit [11] or
351 with low levels of the α3 subunit [45], likely because the α3, α5, and β4 nAChR subunits,
352 which are encoded by the same gene cluster, co-assemble in brain structures, notably
353 the MHb-IPN pathway, to produce functional heteromeric nAChRs that contribute to
354 the control of nicotine intake.
355
356 One important limitation of population-level analyses is that they greatly limit the ability
357 to examine inter-individual differences in drug taking behaviors. It is indeed
358 increasingly acknowledged that in mice, as in humans, there is a substantial variability
359 in the susceptibility for developing drug use disorders [26-28,44-47]. Yet, it is still unclear
360 why some individuals are more susceptible than others to become regular users. Here
361 we inspected drinking profiles in individual isogenic mice, and discovered large inter-

362 individual differences in nicotine vulnerability: about half of the WT mice, the avoiders,
363 durably quit nicotine at a certain dose, whereas the other half, the consumers,
364 continued consumption even at high doses of nicotine, classically described as
365 aversive [2]. Avoiders displayed variable threshold doses for aversion, and some of them
366 even developed aversion at the beginning of the two-bottle choice experiment, when
367 concentrations of nicotine were still low. This finding challenges the popular idea that
368 aversion is only triggered by high doses of nicotine [2,11-13]. By directly measuring the
369 response of IPN neurons to different doses of nicotine *in vivo*, we show that
370 concentrations of nicotine as low as 7.5 μg/kg can engage the IPN circuitry, suggesting
371 that nicotine-induced signaling can emerge in this structure even at low doses of the
372 drug. Consumers (WT and $\beta4^{-/-}$ mice) may still have an aversion threshold that would
373 exceed the highest dose tested here. Importantly, very few mice showed what could
374 be considered as "efficient titration", emphasizing the needs to consider individual
375 behavior, as opposed to group behavior, in addiction research.
376
377 We also discovered that the functional expression level of β4-containing nAChRs in
378 the IPN underlies these different sensitivities to the aversive properties of nicotine.
379 Indeed, inter-individual variability for nicotine aversion was virtually eliminated in $\beta4^{-/-}$
380 mice, none of which quit drinking nicotine, and was restored after selective re-
381 expression of the β4 subunit in the IPN. Strikingly, we observed a negative correlation
382 between nicotine consumption and the response of the IPN to the drug: mice
383 consuming high amounts of nicotine displayed lower nicotine-evoked currents in the
384 IPN than mice consuming small amounts of nicotine, which displayed large currents.
385 The expression level of β4-containing nAChRs in the IPN thus determines the aversion
386 threshold for the drug, and consequently its intake. We suggest that β4-containing

387 nAChRs, by engaging the IPN circuitry, initiate a primary response to nicotine that, if
388 above a certain threshold, will trigger acute aversion to the drug, thus impacting the
389 balance between drug reward and aversion to limit drug consumption. In line with this,
390 it was found that pharmacological or optogenetic stimulation of the MHb-IPN pathway
391 could directly produce aversion [13,14,33], while pharmacological inactivation of this
392 pathway increases nicotine intake [11]. From our results, we further suggest that the
393 aversion produced by nicotine is not just acute but also long-lasting, since mice persist
394 in avoiding nicotine even after the concentration has been lowered to a dose they used
395 to ingest. This echoes observations made in humans, in which the unpleasant initial
396 responses to cigarettes is associated with a reduced likelihood of continued smoking
397 [48]. Such a sustained aversive reaction to nicotine was conditioned, in mice, by nicotine
398 itself, and required β4-containing nAChRs of the IPN for its onset, but most likely
399 involves other brain circuits for its persistence in the long-term. Identifying the
400 molecular and cellular mechanism of long-term aversion to nicotine in mice will be
401 instrumental to progress in our understanding of human dependence to tobacco.
402
403 We did not observe major differences in the consumption levels of avoiders and
404 consumers at the beginning of the two-bottle choice experiment, for low concentrations
405 of nicotine (< 100 μg/ml), but cannot completely rule out pre-existing inter-individual
406 differences that may explain the opposite trajectories taken by the two groups. Indeed,
407 the mice used in this study were isogenic, yet epigenetic changes during development
408 or differences in social status, which are known to affect brain circuits and individual
409 traits [49], may affect the responses of the IPN to nicotine. It is indeed tempting to
410 speculate that external factors (e.g. stress, social interactions…) that would affect the
411 expression level of β4-containing nAChRs in the IPN, will have a strong impact on

412 nicotine consumption. In addition to pre-existing differences, history of nicotine use
413 could produce long-lasting molecular and cellular adaptations in the IPN circuitry that
414 may affect nicotine aversion and consumption. In the VTA, chronic nicotine
415 upregulates the number of β2-containing receptors at the cell surface [50,51]. We
416 discovered that prolonged nicotine exposure had the opposite effect on β4-containing
417 nAChRs of the IPN: it downregulated and/or desensitized these receptors, as
418 evidenced by the decreased response to nicotine both *ex-vivo* and *in-vivo*. This effect
419 seems to be specific to β4-containing nAChRs, since chronic nicotine had virtually no
420 consequence on the residual IPN nAChR current in $\beta4^{-/-}$ mice. These results may
421 appear at odds with the recent report of increased nAChR currents in IPN slices of
422 nicotine-treated mice [52]. Nevertheless, our behavioral results in nicotine-treated WT
423 and $\beta4^{-/-}$ mice completely match: both displayed reduced responses to nicotine (ex vivo
424 and i*n vivo)* in IPN neurons, as well as increased nicotine consumption compared to
425 naive, WT animals. We suggest that long-term exposure to nicotine increases the
426 threshold for aversion to the drug, and thereby increases drug consumption. In other
427 words, nicotine intake history weakens the ability of nicotine to induce aversion in mice.
428 In most nicotine replacement therapies, such as gums or patches, nicotine is slowly
429 administered over prolonged periods of time, to supposedly attenuate the negative
430 emotional reactions elicited by nicotine withdrawal. However, we show that mice under
431 prolonged nicotine administration will also develop tolerance to the aversive effects of
432 nicotine, thus providing some possible explanation as to why such replacement
433 strategies in humans have limited efficacy in the long term [53], and highlighting the
434 necessity to develop alternative medical approaches.

435 **Materials and Methods**

436 *Animals*

437 Eight to sixteen-week old wild-type C57BL/6J (Janvier labs, France) and Acnb4 knock-
438 out ($\beta4^{-/-}$) mice (Pasteur Institute, Paris) [54] were used for this study. $\beta4^{-/-}$ mice were
439 backcrossed onto C57BL/6J background for more than twenty generations. Mice were
440 maintained on a 12h light and dark cycle. All experiments were performed in
441 accordance with the recommendations for animal experiments issued by the European
442 Commission directives 219/1990, 220/1990 and 2010/63, and approved by Sorbonne
443 Université.

444

445 *Two-bottle choice experiment*

446 Mice single-housed in a home cage were presented with two bottles of water (Volvic)
447 for a habituation period of 4 days. After habituation, mice were presented with one
448 bottle of saccharine solution (2%, Sigma Aldrich) and one bottle of nicotine (free base,
449 Sigma Aldrich) plus saccharine (2%) solution diluted in water (adjusted to pH ~7.2 with
450 NaOH). Unless otherwise noted, four different concentrations of nicotine were tested
451 consecutively (10, 50, 100 and 200 µg/ml) with changes in concentration occurring
452 every 4 days. For the two-bottle aversion task, a single nicotine concentration (100
453 µg/ml) was used after the habituation period. Bottles were swapped every other day to
454 control for side preference. The drinking volume was measured every minute with an
455 automated acquisition system (TSE system, Germany). Mice were weighed every
456 other day to quantify the nicotine intake in mg/kg/day. Mice showing a strong side bias
457 (preference <20% or >80%) in the habituation period were not taken into account for
458 the analyses.

459 For the pseudo-ternary plot analyses, mouse choices (each drinking event) were
460 quantified using the percentage of choices for the nicotine-containing bottle. For each
461 dose of nicotine and each animal, we calculated two percentages, associated with
462 nicotine on the left-hand side (%c1) and nicotine on the right-hand side (%c2),
463 respectively. To evaluate avoidance of nicotine, tracking or side bias, we plotted
464 min(%c1, %c2) against max(%c1, %c2). In this plot the three summits (0,0), (1,1) and
465 (0,1) represent mice that avoid nicotine on both sides, mice that track nicotine on both
466 sides, and finally mice that drink only one side, respectively. We then used a 90°
467 rotation to obtain the pseudo-ternary plot.
468
469 *Prolonged treatment with nicotine*
470 Osmotic minipumps (2004, Alzet minipump) were implanted subcutaneously in 8-
471 week-old mice anesthetized with isoflurane (1%). Minipumps continuously delivered
472 nicotine (10 mg/kg/d) or saline (control) solution with a rate of 0.25 µl/h during 4 weeks.
473
474 *Brain slice preparation*
475 Mice were weighed and then anaesthetized with an intraperitoneal injection of a
476 mixture of ketamine (150 mg/kg, Imalgene 1000, Merial, Lyon, France) and xylazine
477 (60 mg/kg, Rompun 2%, Bayer France, Lyon, France). Blood was then fluidized by an
478 injection of an anticoagulant (0.1mL, heparin 1000 U/mL, Sigma) into the left ventricle,
479 and an intra-cardiac perfusion of ice-cold (0-4°C), oxygenated (95% O_2/5% CO_2)
480 sucrose-based artificial cerebrospinal fluid (SB-aCSF) was performed. The SB-aCSF
481 solution contained (in mM): 125 NaCl, 2.5 KCl, 1.25 NaH_2PO_4, 5.9 $MgCl_2$, 26 $NaHCO_3$,
482 25 sucrose, 2.5 glucose, 1 kynurenate (pH 7.2). After rapid brain sampling, slices (250
483 µm thick) were cut in SB-aCSF at 0-4°C using a Compresstome slicer (VF-200,

484 Precisionary Instruments Inc.). Slices were then transferred to the same solution at
485 35°C for 10 min, then moved and stored in an oxygenated aCSF solution at room
486 temperature. The aCSF solution contained in mM: 125 NaCl, 2.5 KCl, 1.25 NaH_2PO_4,
487 2 $CaCl_2$, 1 $MgCl_2$, 26 $NaHCO_3$, 15 sucrose, 10 glucose (pH 7.2). After minimum 1h of
488 rest, slices were placed individually in a recording chamber at room temperature and
489 infused continuously with aCSF recording solution at a constant flow rate of about 2
490 ml/min.
491
492 *Ex vivo patch-clamp recordings of IPN neurons*
493 Patch pipettes (5-8 MΩ) were stretched from borosilicate glass capillaries (G150TF-3,
494 Warner instruments) using a pipette puller (Sutter Instruments, P-87, Novato, CA) and
495 filled with a few microliters of an intracellular solution adjusted to a pH of 7.2, containing
496 (in mM): 116 K-gluconate, 20 HEPES, 0.5 EGTA, 6 KCl, 2 NaCl, 4 ATP, 0.3 GTP and
497 2 mg/mL biocytin. Biocytin was used to label recorded neurons. The slice of interest
498 was placed in the recording chamber and viewed using a white light source and a
499 straight microscope coupled to a Dodt contrast lens (Scientifica, Uckfield, UK).
500 Neurons were recorded from the dorsal (IPDL) and rostral (IPR) parts on the IPN.
501 Whole-cell configuration recordings of IPN neurons were performed using an amplifier
502 (Axoclamp 200B, Molecular Devices, Sunnyvale, CA) connected to a digitizer (Digidata
503 1550 LowNoise acquisition system, Molecular Devices, Sunnyvale, CA). Signal
504 acquisition was performed at 10 kHz, filtered with a lowpass (Bessel, 2 kHz) and
505 collected by the acquisition software pClamp 10.5 (Molecular Devices, Sunnyvale,
506 CA). Nicotine tartrate (30 μM in aCSF) was locally and briefly applied (200 ms puffs)
507 using a puff pipette (glass pipette ~3 μm diameter at the tip) positioned about 20-30
508 μm from the soma of the neuron. The pipette was connected to a Picospritzer (PV-800

509 PicoPump, World Precision Instruments) controlled with pClamp to generate transient
510 pressure in the pipette (~2 psi). Nicotine-evoked currents were recorded in voltage-
511 clamp mode at a membrane potential of -60 mV. All electrophysiology traces were
512 extracted and pre-processed using Clampfit (Molecular Devices, Sunnyvale, CA) and
513 analyzed with R.
514
515 *In vivo electrophysiology*
516 Mice were deeply anesthetized with chloral hydrate (8%, 400 mg/kg) and anesthesia
517 was maintained throughout the experiment with supplements. Catheters were
518 positioned in the saphenous veins of the mice to perform saline or nicotine intravenous
519 injections. Nicotine hydrogen tartare salt (Sigma-Aldrich) was dissolved in 0.9% NaCl
520 solution and pH was adjusted to 7.4. The nicotine solution was injected at a dose of
521 7.5, 15 and 30 µg/kg. Borosilicate glass tubings (1.5 mm O.D. / 1.17 mm I.D., Harvard
522 Apparatus) were pulled using a vertical puller (Narishige). Glass pipettes were broken
523 under a microscope to obtain a ~1 µm diameter at the tip. Electrodes were filled with
524 a 0.5% NaCl solution containing 1.5% of neurobiotin tracer (AbCys) yielding
525 impedances of 6-9 MΩ. Electrical signals were amplified by a high-impedance amplifier
526 (Axon Instruments) and supervised through an audio monitor (A.M. Systems Inc.). The
527 signal was digitized, sampled at 25 kHz and recorded on a computer using Spike2
528 (Cambridge Electronic Design) for later analysis. IPN neurons were recorded in an
529 area corresponding to the following stereotaxic coordinates (4-5° angle): 3.3 - 3.6 mm
530 posterior to bregma, 0.2 - 0.45 mm from medial to lateral and 4.3 - 5 mm below the
531 brain surface. A 5 min-baseline was recorded prior to saline or nicotine i.v. injection.
532 For the dose-response experiments, successive randomized injections of nicotine (or

533 saline) were performed, interspaced with sufficient amount of time (> 10 min) to allow
534 the neuron to return to its baseline.
535
536 *Stereotaxic viral injections*
537 8-week old mice were injected in the IPN with a lentivirus that co-expresses the WT β4
538 subunit together with eGFP (or only eGFP for control experiments) under the control
539 of the PGK promoter. Lentiviruses were produced as previously described [6]. For viral
540 transduction, mice were anaesthetized with a gas mixture containing 1-3% isoflurane
541 (IsoVet®, Pyramal Healthcare Ltd., Nothumberland, UK) and placed in a stereotactic
542 apparatus (David Kopf Instruments, Tujunga, CA). Unilateral injections (0.1µl/min) of
543 1µl of a viral solution (Lenti.pGK.β4.IRES.eGFP, titer 150 ng/µl of p24 protein; or
544 Lenti.pGK.eGFP, titer 75 ng/µl of p24 protein) were performed using a cannula
545 (diameter 36G, Phymep, Paris, France). The cannula was connected to a Hamilton
546 syringe of 10 µL (Model 1701, Hamilton Robotics, Bonaduz, Switzerland) placed in a
547 syringe pump (QSI, Stoelting Co, Chicago, IL, USA). Injections were performed in the
548 IPN at the following coordinates (5° angle): from bregma ML - 0.4 mm, AP - 3.5 mm,
549 and DV: - 4.7 mm (according to Paxinos & Franklin). Electrophysiological recordings
550 were made at least 4 weeks after injection, the time required for the expression of the
551 transgene, and proper expression was subsequently checked using
552 immunohistochemistry.
553
554 *Immunocytochemical identification*
555 Immunostaining was performed as described in [9], *with the following* primary antibodies:
556 anti-tyrosine hydroxylase 1:500 (anti-TH, Sigma, T1299) and chicken anti-eYFP 1:500
557 (Life technologies Molecular Probes, A-6455). Briefly, serial 60 µm-thick sections of

558 the midbrain were cut with a vibratome. Slice were permeabilized for one hour in a
559 solution of phosphate-buffered saline (PBS) containing 3% bovine serum albumin
560 (BSA, Sigma; A4503). Sections were incubated with primary antibodies in a solution
561 of 1.5 % BSA and 0.2 % Triton X-100 overnight at 4℃, washed with PBS and then
562 incubated with the secondary antibodies for 1 hour. The secondary antibodies were
563 Cy3-conjugated anti-mouse (1:500 dilution) and alexa488-conjugated anti-chicken
564 secondary (1:1000 dilution) (Jackson ImmunoResearch, 715-165-150 and 711-225-
565 152, respectively). For the juxtacellular immunostaining, the recorded neurons were
566 identified with the addition of AMCA-conjugated streptavidin (1:200 dilution) in the
567 solution (Jackson ImmunoResearch). Slices were mounted using Prolong Gold
568 Antifade Reagent (Invitrogen, P36930). Microscopy was carried out either with a
569 confocal microscope (Leica) or with an epifluorescence microscope (Leica), and
570 images were captured using a camera and analyzed with ImageJ.
571
572 *Statistical analyses.*
573 All statistical analyses were computed using R (The R Project, version 4.0.0). Results
574 were plotted as a mean ± s.e.m. The total number (n) of observations in each group
575 and the statistics used are indicated in figure legends. Classical comparisons between
576 means were performed using parametric tests (Student's T-test, or ANOVA for
577 comparing more than two groups when parameters followed a normal distribution
578 (Shapiro test $P > 0.05$), and non-parametric tests (here, Mann-Whitney or Friedman)
579 when the distribution was skewed. Multiple comparisons were corrected using a
580 sequentially rejective multiple test procedure (Holm-Bonferroni correction). All
581 statistical tests were two-sided. $P > 0.05$ was considered not to be statistically
582 significant.

583

584 **Author contribution**: SM and RDC performed patch-clamp recordings; SM, CN, ST
585 and FM performed juxtacellular recordings; SM and CN performed stereotaxic
586 injections; SM, EV, CN and JJ performed behavioral tests; NT and SM developed
587 analytical tools; SM and CN performed immunostainings, SP and UM provided viral
588 tools and transgenic lines; SM, PF and AM designed the study; PF and AM acquired
589 funding; SM, PF and AM wrote the article, with inputs from the other authors.

590

591 **Acknowledgments**: The authors would like to thank Ines Centeno-Lemaire (Sorbonne
592 Université, Paris, France) for her help with behavioral tests, Jean-Pierre Hardelin
593 (ESPCI, Paris, France) for critical reading of the manuscript, and the animal facility at
594 Institut de Biology Paris Seine (IBPS, Paris, France). This work was supported by the
595 Agence Nationale de la Recherche (ANR-21-CE16-0012 CHOLHAB to A.M.), by the
596 Fondation pour la Recherche Médicale (Equipe FRM DEQ2013326488 to P.F.), by the
597 Institut National du Cancer Grant TABAC-16-022 and TABAC-19-02 (to P.F.). A.M.
598 was recipient of a fundamental research prize from the Fondation Médisite for
599 neuroscience. S.M. and R.D.C. were supported by a fourth-year fellowship from FRM
600 (FDT201904008060 and FDT20170437427). CN was supported by a fourth-year
601 fellowship from the Biopsy Labex. JJ was supported by a fourth-year fellowship from
602 the Memolife Labex. All data needed to evaluate the conclusions in the paper are
603 present in the paper and/or the Supplementary materials.

604

605 **Competing interests**: The authors declare no competing interest.

606 **References**

607

608 1. *WHO global report on trends in prevalence of tobacco use 2000-2025 third*
609 *edition*. 1–121 (2019).

610 2. Fowler, C. D. & Kenny, P. J. Nicotine aversion: Neurobiological mechanisms and
611 relevance to tobacco dependence vulnerability. *Neuropharmacology* **76 Pt B,**
612 533–544 (2014).

613 3. Verendeev, A. & Riley, A. L. The role of the aversive effects of drugs in self-
614 administration. *Behavioural Pharmacology* **24,** 363–374 (2013).

615 4. Taly, A., Corringer, P.-J., Guedin, D., Lestage, P. & Changeux, J.-P. Nicotinic
616 receptors: allosteric transitions and therapeutic targets in the nervous system.
617 *Nat Rev Drug Discov* **8,** 733–750 (2009).

618 5. Zoli, M., Pistillo, F. & Gotti, C. Diversity of native nicotinic receptor subtypes in
619 mammalian brain. *Neuropharmacology* **96,** 302–311 (2015).

620 6. Maskos, U. *et al.* Nicotine reinforcement and cognition restored by targeted
621 expression of nicotinic receptors. *Nature* **436,** 103–107 (2005).

622 7. Tapper, A. R. *et al.* Nicotine activation of alpha4* receptors: sufficient for reward,
623 tolerance, and sensitization. *Science* **306,** 1029–1032 (2004).

624 8. Tolu, S. *et al.* Co-activation of VTA DA and GABA neurons mediates nicotine
625 reinforcement. *Mol Psychiatry* **18,** 382–393 (2013).

626 9. Durand-de Cuttoli, R. *et al.* Manipulating midbrain dopamine neurons and
627 reward-related behaviors with light-controllable nicotinic acetylcholine receptors.
628 *eLife* **7,** 15991 (2018).

629 10. Nguyen, C. *et al.* Nicotine inhibits the VTA-to-amygdala dopamine pathway to
630 promote anxiety. *Neuron* **109,** 2604–2615.e9 (2021).

631 11. Fowler, C. D., Lu, Q., Johnson, P. M., Marks, M. J. & Kenny, P. J. Habenular α5
632 nicotinic receptor subunit signalling controls nicotine intake. *Nature* **471,** 597–
633 601 (2011).
634 12. Frahm, S. *et al.* Aversion to Nicotine Is Regulated by the Balanced Activity of
635 beta4 and alpha5 Nicotinic Receptor Subunits in the Medial Habenula. *Neuron*
636 **70,** 522–535 (2011).
637 13. Wolfman, S. L. *et al.* Nicotine aversion is mediated by GABAergic
638 interpeduncular nucleus inputs to laterodorsal tegmentum. *Nature*
639 *Communications* **9,** 2710 (2018).
640 14. Morton, G. *et al.* Chrna5-Expressing Neurons in the Interpeduncular Nucleus
641 Mediate Aversion Primed by Prior Stimulation or Nicotine Exposure. *J. Neurosci.*
642 **38,** 6900–6920 (2018).
643 15. Otsu, Y. *et al.* Control of aversion by glycine-gated GluN1/GluN3A NMDA
644 receptors in the adult medial habenula. *Science* **366,** 250–254 (2019).
645 16. Yamaguchi, T., Danjo, T., Pastan, I., Hikida, T. & Nakanishi, S. Distinct Roles of
646 Segregated Transmissionof the Septo-Habenular Pathway in Anxiety and Fear.
647 *Neuron* **78,** 537–544 (2013).
648 17. Zhang, J. et al. (2016). Presynaptic Excitation via GABAB Receptors in
649 Habenula Cholinergic Neurons Regulates Fear Memory Expression. *Cell* **166,**
650 716–728 (2016).
651 18. Salas, R., Sturm, R., Boulter, J. & De Biasi, M. Nicotinic Receptors in the
652 Habenulo-Interpeduncular System Are Necessary for Nicotine Withdrawal in
653 Mice. *J. Neurosci.* **29,** 3014–3018 (2009).

654 19. Zhao-Shea, R. *et al.* Increased CRF signalling in a ventral tegmentalarea-
655 interpeduncular nucleus-medial habenulacircuit induces anxiety during nicotine
656 withdrawal. *Nature Communications* **6,** 1–13 (2015).
657 20. Pang, X. *et al.* Habenula cholinergic neurons regulate anxiety during nicotine
658 withdrawal via nicotinic acetylcholine receptors. *Neuropharmacology* **107,** 294–
659 304 (2016).
660 21. Zhao-Shea, R., Liu, L., Pang, X., Gardner, P. D. & Tapper, A. R. Activation of
661 GABAergic Neuronsin the Interpeduncular Nucleus Triggers Physical Nicotine
662 Withdrawal Symptoms. *Current Biology* **23,** 2327–2335 (2013).
663 22. Forget, B. *et al.* A Human Polymorphism in CHRNA5 Is Linked to Relapse to
664 Nicotine Seeking in Transgenic Rats. *Curr. Biol.* **28,** 3244–3253.e7 (2018).
665 23. Bierut, L. J. *et al.* Variants in nicotinic receptors and risk for nicotine dependence.
666 *Am J Psychiatry* **165,** 1163–1171 (2008).
667 24. Lassi, G. *et al.* The CHRNA5–A3–B4 GeneCluster and Smoking: FromDiscovery
668 to Therapeutics. *Trends in Neurosciences* **39,** 851–861 (2016).
669 25. George, O. & Koob, G. F. Individual differences in the neuropsychopathology of
670 addiction. *Dialogues Clin Neurosci* **19,** 217–229 (2017).
671 26. Deroche-Gamonet, V., Belin, D. & Piazza, P. V. Evidence for addiction-like
672 behavior in the rat. *Science* **305,** 1014–1017 (2004).
673 27. Siciliano, C. A. *et al.* A cortical-brainstem circuit predicts and governs compulsive
674 alcohol drinking. *Science* **366,** 1008–1012 (2019).
675 28. Juarez, B. *et al.* Midbrain circuit regulation of individual alcohol drinking
676 behaviors in mice. *Nature Communications* **8,** 2220 (2017).
677 29. Pascoli, V. *et al.* Stochastic synaptic plasticity underlying compulsion in a model
678 of addiction. *Nature* **564,** 1–22 (2018).

679 30. Centers for Disease Control and Prevention (US), National Center for Chronic
680 Disease Prevention and Health Promotion (US)Office on Smoking and Health
681 (US). How Tobacco Smoke Causes Disease: The Biology and Behavioral Basis
682 for Smoking-Attributable Disease: A Report of the Surgeon General. (2010).
683 31. Harrington, L. *et al.* Role of β4* Nicotinic Acetylcholine Receptors in the
684 Habenulo-Interpeduncular Pathway in Nicotine Reinforcement in Mice.
685 *Neuropsychopharmacology* **41,** 1790–1802 (2016).
686 32. Husson, M. *et al.* β4-Nicotinic Receptors Are Critically Involved in Reward-
687 Related Behaviors and Self-Regulation of Nicotine Reinforcement. *J. Neurosci.*
688 **40,** 3465–3477 (2020).
689 33. Tuesta, L. M. *et al.* GLP-1 acts on habenular avoidance circuits to control
690 nicotine intake. *Nature Neuroscience* **20,** 708–716 (2017).
691 34. Antolin-Fontes, B. *et al.* The habenular G-protein-coupled receptor 151 regulates
692 synaptic plasticity and nicotine intake. *Proceedings of the National Academy of*
693 *Sciences* **117,** 5502–5509 (2020).
694 35. Molas, S., DeGroot, S. R., Zhao-Shea, R. & Tapper, A. R. Anxiety and Nicotine
695 Dependence: Emerging Role of the Habenulo-Interpeduncular Axis. *Trends in*
696 *Pharmacological Sciences* **38,** 169–180 (2017).
697 36. McLaughlin, I., Dani, J. A. & De Biasi, M. The medial habenula and
698 interpeduncular nucleus circuitry is critical in addiction, anxiety, and mood
699 regulation. *J Neurochem* **142,** 130–143 (2017).
700 37. Hsu, Y.-W. A. *et al.* Medial habenula output circuit mediated by α5 nicotinic
701 receptor-expressing GABAergic neurons in the interpeduncular nucleus. *J.*
702 *Neurosci.* **33,** 18022–18035 (2013).

703 38. Quina, L. A., Harris, J., Zeng, H. & Turner, E. E. Specific connections of the
704 interpeduncular subnuclei reveal distinct components of the
705 habenulopeduncular pathway. *J. Comp. Neurol.* **525,** 2632–2656 (2017).
706 39. Fenster, C. P., Rains, M. F., Noerager, B., Quick, M. W. & Lester, R. A. Influence
707 of subunit composition on desensitization of neuronal acetylcholine receptors at
708 low concentrations of nicotine. *J. Neurosci.* **17,** 5747–5759 (1997).
709 40. Shih, P.-Y. *et al.* Differential Expression and Function of Nicotinic Acetylcholine
710 Receptors in Subdivisions of Medial Habenula. *J. Neurosci.* **34,** 9789–9802
711 (2014).
712 41. Grady, S. R. *et al.* Rodent habenulo-interpeduncular pathway expresses a large
713 variety of uncommon nAChR subtypes, but only the alpha3beta4* and
714 alpha3beta3beta4* subtypes mediate acetylcholine release. *J. Neurosci.* **29,**
715 2272–2282 (2009).
716 42. Pogun, S. & C Collins, A. Oral Nicotine Self-Administration in Rodents. *J Addict*
717 *Res Ther* **01,** 1–19 (2012).
718 43. Gallego, X. *et al.* Overexpression of the CHRNA5/A3/B4 genomic cluster in mice
719 increases the sensitivity to nicotine and modifies its reinforcing effects. *Amino*
720 *Acids* **43,** 897–909 (2011).
721 44. Nesil, T., Kanit, L., Collins, A. C. & Pogun, S. Individual differences in oral
722 nicotine intake in rats. *NP* **61,** 189–201 (2011).
723 45. Garcia-Rivas, V., Cannella, N. & Deroche-Gamonet, V. Individual Variations in
724 the Mechanisms of Nicotine Seeking: A Key for Research on Nicotine
725 Dependence. *Neuropsychopharmacology* **42,** 584–586 (2017).

726 46. Piazza, P. V., Deminière, J. M., Le Moal, M. & Simon, H. Factors that predict
727 individual vulnerability to amphetamine self-administration. *Science* **245,** 1511–
728 1513 (1989).
729 47. Dongelmans, M. *et al.* Chronic nicotine increases midbrain dopamine neuron
730 activity and biases individual strategies towards reduced exploration in mice.
731 *Nature Communications* **12,** 6945 (2021).
732 48. DiFranza, J. R. *et al.* Recollections and repercussions of the first inhaled
733 cigarette. *Addictive Behaviors* **29,** 261–272 (2004).
734 49. Torquet, N. *et al.* Social interactions impact on the dopaminergic system and
735 drive individuality. *Nature Communications* **9,** 3081 (2018).
736 50. Sallette, J. *et al.* Nicotine Upregulates Its Own Receptors through Enhanced
737 Intracellular Maturation. *Neuron* **46,** 595–607 (2005).
738 51. Lester, H. A. *et al.* Nicotine is a Selective Pharmacological Chaperone of
739 Acetylcholine Receptor Number and Stoichiometry. Implications for Drug
740 Discovery. *AAPS J* **11,** 167–177 (2009).
741 52. Arvin, M. C., Yan, Y., Beckley, N. A., Henry, B. A. & Drenan, R. M. Chronic
742 nicotine exposure alters the neurophysiology of habenulo-interpeduncular
743 circuitry. *J. Neurosci.* 2816–18–52 (2019). doi:10.1523/JNEUROSCI.2816-
744 18.2019
745 53. Hartmann-Boyce, J., Chepkin, S. C., Ye, W., Bullen, C. & Lancaster, T. Nicotine
746 replacement therapy versus control for smoking cessation. *Cochrane Database*
747 *of Systematic Reviews* **1,** 7–196 (2018).
748 54. Xu, W. *et al.* Multiorgan autonomic dysfunction in mice lacking the beta2 and the
749 beta4 subunits of neuronal nicotinic acetylcholine receptors. *J. Neurosci.* **19,**
750 9298–9305 (1999).

751 **Figure Legends**

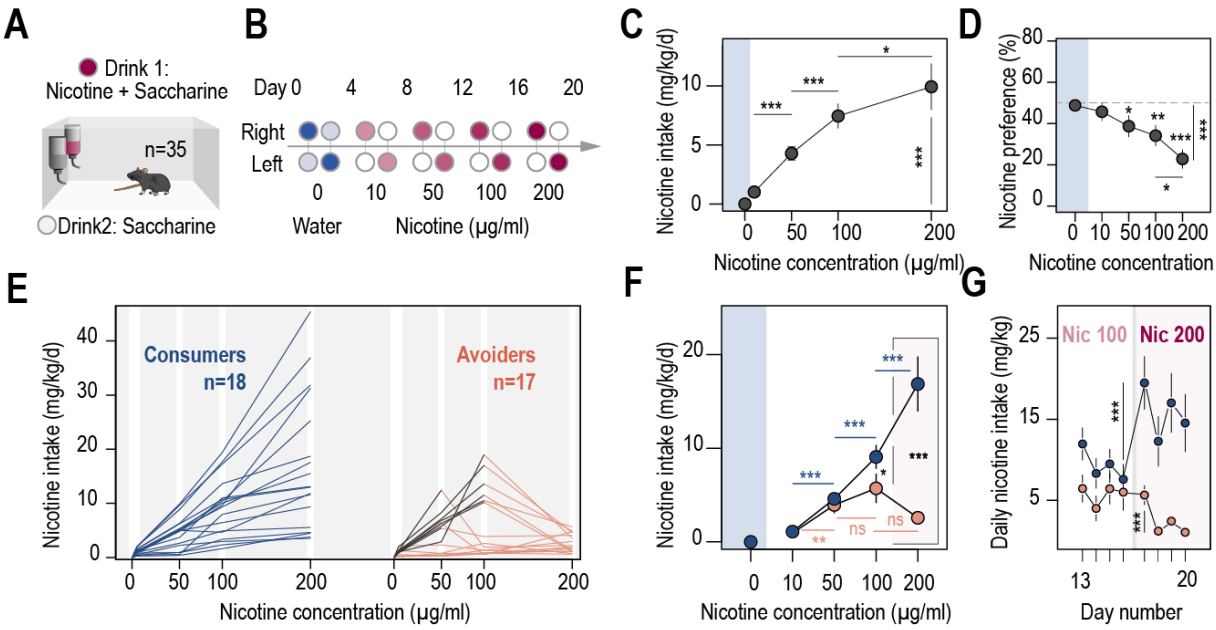

752 **FIGURE 1**

753 **Figure 1: Two different profiles, consumers and avoiders, emerged in WT mice**
754 **subjected to a two-bottle choice nicotine-drinking test. A.** Continuous access, two-
755 bottle choice setup. **B.** Two-bottle choice paradigm. Each dot represents a bottle and
756 is color-coded according to whether it contains water (blue or light blue), nicotine plus
757 2% saccharine (red, gradient of color intensities according to the concentration), or 2%
758 saccharine (white) solutions. The nicotine concentration in the bottle increased
759 progressively from 10 to 50, 100 and 200 µg/ml. Each condition lasted 4 days, and the
760 bottles were swapped every other day. **C.** Daily nicotine intake (mg/kg/d) averaged
761 over four days, as a function of nicotine concentration in the bottle (Friedman test, n =
762 35, df = 3, $p < 0.001$ and Mann-Whitney post-hoc test with Holm-Bonferroni correction).
763 **D.** Nicotine preference (%) in WT mice for each dose of nicotine, averaged over four
764 days (Friedman test, n = 35, df = 4, $p < 0.001$ and Mann-Whitney post-hoc test with
765 Holm-Bonferroni correction) **E.** Nicotine intake in individual consumers (n = 18) and
766 avoiders (n = 17). **F.** Nicotine consumption in consumers and avoiders for each nicotine

767 dose, averaged over four days (Mann-Whitney comparison with a Holm-Bonferroni
768 correction). **G.** Daily nicotine consumption in consumers and avoiders for the nicotine
769 100 and 200 μg/ml conditions. Note the drop in nicotine consumption at day 2 of
770 nicotine 200 μg/ml for avoiders. In all figure panels avoiders are depicted in pinkish-
771 orange while consumers are in blue (paired Mann-Whitney). *** $p < 0.001$, ** $p < 0.01$,
772 * $p < 0.05$.

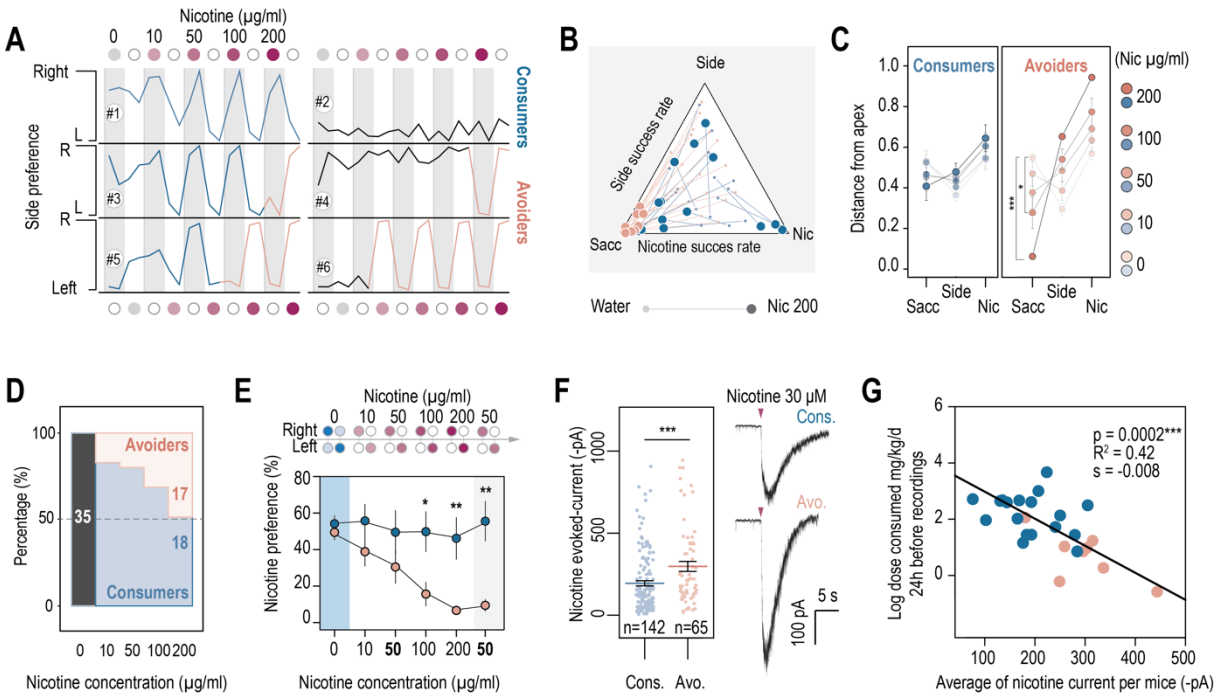

FIGURE 2

Figure 2: Nicotine consumption was negatively correlated with the amplitude of the response to nicotine in IPN neurons. A. Representative examples of choice behaviors in WT mice when the right-hand side bottle contains either nicotine + saccharine (red dots, grey stripe) or saccharine only (white dots, white stripes). Consumers maintained their strategy throughout the 20-day long test, and either tracked the side associated with nicotine (e.g. mouse #1) or had a strong side bias (e.g. mouse #2). Avoiders actively avoided the side associated with nicotine after a certain nicotine dose was reached in the bottle, whether they initially tracked nicotine (e.g. mice #3 or 5) or not (e.g. mice # 4 or 6). Mice are same as in Fig. 1. **B.** Pseudo-ternary diagram representing, for each individual (18 consumers and 17 avoiders, see figure 1), its side success rate over its nicotine success rate. Bottom left apex: 100% saccharine preference (Sacc); Bottom right apex: 100% nicotine preference (Nic); Top apex: 100% side preference (Side, absolute non-switchers). Small dots correspond to the habituation period (water vs. water) while bigger dots correspond to the condition

788 with 200 µg/ml of nicotine in one bottle. Note how all avoider mice end up in the bottom
789 left apex (0% nicotine preference) at the end of the task. **C.** Average distance from the
790 three apices for each condition in the task (0, 10, 50, 100 and 200 µg/ml of nicotine,
791 color-coded from light to dark), for consumers and avoiders. Only avoider mice
792 significantly changed their drinking strategy as nicotine concentration increased
793 (paired Mann-Whitney test with Holm-Bonferroni correction). **D.** Proportion of avoiders
794 and consumers as nicotine concentration increases. **E.** Average nicotine preference
795 (%) for avoider and consumer mice for each dose of nicotine in the two-bottle choice
796 task. The 50 µg/ml nicotine solution was presented a second time to the mice, at the
797 end of the session. (Mann-Whitney test, Holm-Bonferroni correction, p(50 Nic) = 0.04,
798 p(100 Nic) = 0.005, p(200 Nic) = 0.004). **F.** Representative (right) and average (left)
799 currents recorded in voltage-clamp mode (-60 mV) from IPN neurons of consumers
800 (blue, n = 142, -194 ± 15 pA) and avoiders (red, n = 65, -297 ± 30 pA) following a puff
801 application of nicotine (30 µM, 200 ms). Avoiders presented greater nicotine-evoked
802 currents than consumers (Mann-Whitney test, p = 1.4e-11). **G.** Correlation between
803 the dose consumed (log scale, over the last 24 hours prior to the recording) and the
804 averaged nicotine evoked-current per mouse (-pA). In all figure panels avoiders are
805 depicted in pinkish-orange and consumers in blue. *** p<0.001, ** p<0.01, * p<0.05.
806

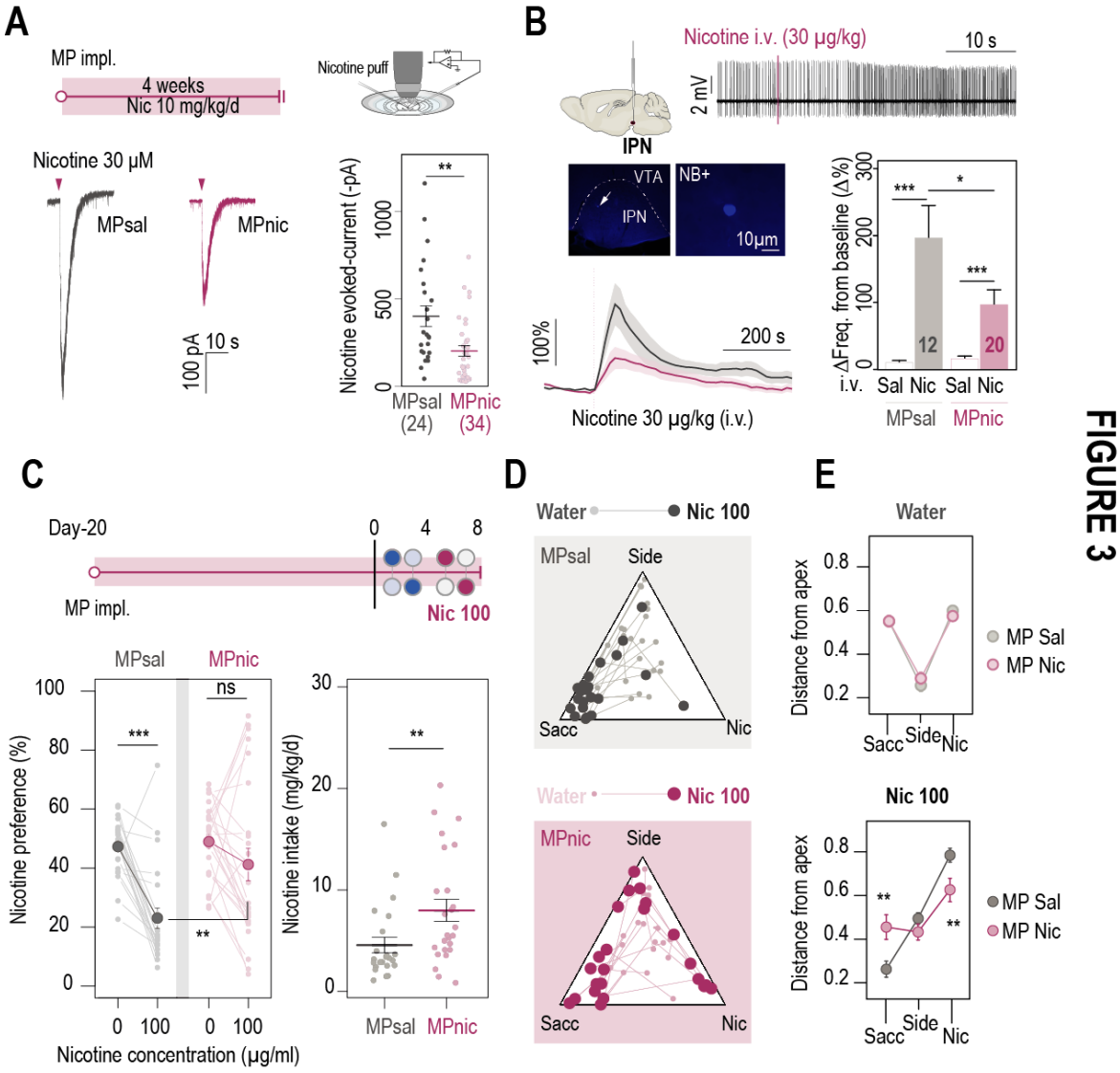

FIGURE 3

Figure 3: Chronic nicotine treatment alters both nAChR expression levels in the IPN and nicotine consumption in WT mice. A. Top, passive nicotine treatment protocol. Mice were implanted subcutaneously with an osmotic minipump (MP) that continuously delivered 10 mg/kg/d of nicotine. After 4 weeks of treatment, nicotine-evoked responses in IPN neurons were recorded in whole-cell voltage-clamp mode (-60 mV) from IPN slices. Bottom, representative recordings (left) and average current amplitudes (right) following a puff application of nicotine (30 µM, 200 ms) in IPN neurons of mice treated either with saline (n = 24, -401 ± 59 pA) or nicotine (n = 34, -202 ± 37 pA). Nicotine treatment reduced the amplitude of nicotine-evoked currents in IPN neurons (Mann-Whitney test, p = 0.001). **B.** *In vivo* juxtacellular recordings of

818 nicotine-evoked responses in IPN neurons of saline- and nicotine-treated animals.
819 Top, representative electrophysiological recording of an IPN neuron, during an i.v.
820 injection of nicotine (30 µg/kg). Middle, post-recording identification of neurobiotin-
821 labeled IPN neurons by immunofluorescence. Bottom, average time course and
822 average amplitude of the change in firing frequency from baseline after an i.v. injection
823 of saline and nicotine (30µg/kg), for IPN neurons from saline- and nicotine-treated
824 mice. Right, firing rate variation from baseline induced by nicotine or saline injection in
825 IPN neurons from saline- or nicotine-treated animals. Responses were decreased by
826 the chronic exposure to nicotine ($p = 0.035$, Mann-Whitney test). All neurons were
827 confirmed to be located within the IPN using juxtacellular labeling with neurobiotin. **C.**
828 Top, modified two-bottle choice protocol used to evaluate the impact of a long-term
829 exposure to nicotine on their nicotine intake. Mice were implanted subcutaneously with
830 a minipump that delivered 10 mg/kg/d of nicotine continuously 20 days before
831 performing the modified two-bottle choice task. After four days of water vs. water
832 habituation, mice were directly exposed to a high concentration of nicotine (100 µg/ml).
833 Bottom, nicotine preference and consumption at 0 and 100 µg/ml of nicotine, for mice
834 under a chronic treatment of nicotine or saline. The saline group displayed a higher
835 avoidance-like behavior ($n = 23$, from $47.3 \pm 2.0\%$ to $23.0 \pm 3.4\%$, $p = 1.7e-05$, Mann-
836 Whitney paired test) than the nicotine group ($n = 25$, from 48.9 ± 2.4 to $41.2 \pm 5.5\%$, p
837 $= 0.16$, Mann-Whitney paired test), leading to lower nicotine consumption ($p = 0.004$
838 and 0.003, Mann-Whitney in nicotine condition for nicotine intake and nicotine
839 preference, respectively). **D.** Pseudo-ternary diagrams representing each saline- and
840 nicotine-treated mouse for its side success rate over its nicotine success rate. Small
841 dots correspond to the habituation period (water vs. water) and bigger dots to the
842 condition with 100 µg/ml of nicotine in one bottle. **E.** Average distance from each apex

843 in the water vs. water (top) and water vs. nicotine 100 μg/ml conditions (bottom).
844 Saline-treated mice developed a strategy to avoid nicotine, but not nicotine-treated
845 mice ($p_{Sacc} = 0.013$, $p_{Side} = 0.27$ $p_{Nic} = 0.013$, Mann-Whitney test with Holm-Bonferroni
846 correction). In all figure panels nicotine-treated animals are displayed in red and saline-
847 treated (control) animals in grey.
848

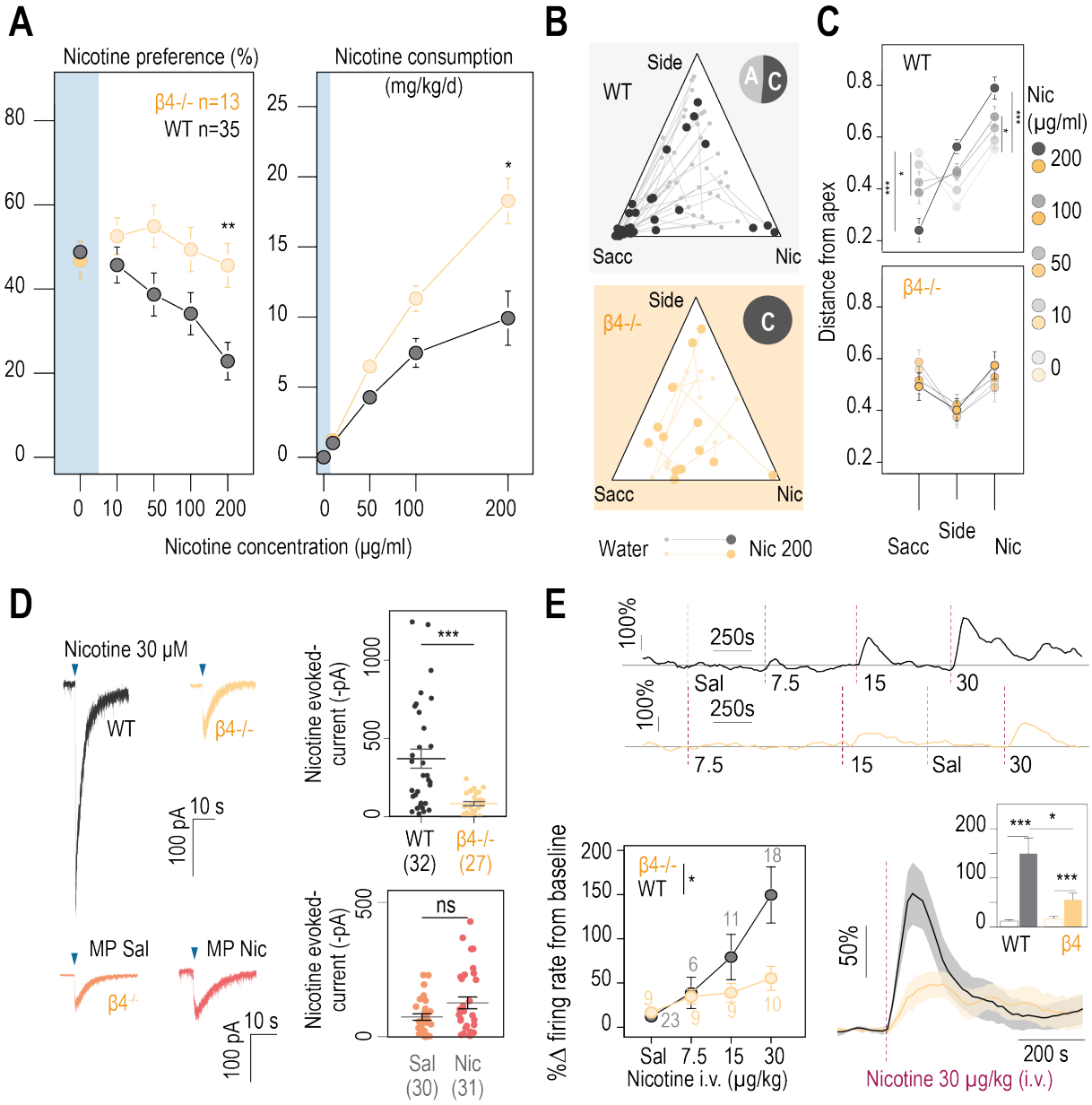

FIGURE 4

Figure 4: β4-containing nicotinic receptors are essential for triggering nicotine avoidance-like behavior in mice. A. Left, average nicotine preference (%) in WT and β4-/- mice for each dose of nicotine in the two-bottle choice task. WT mice decreased their nicotine preference (Friedman test, n = 35, df = 4, $p < 0.001$ and Mann-Whitney post-hoc test with Holm-Bonferroni correction) while $\beta4^{-/-}$ mice displayed a stable preference throughout the task (Friedman test, n = 13, df = 4, p = 0.11). WT mice avoided the nicotine-containing bottle more than $\beta4^{-/-}$ mice (Mann-Whitney test with

857 Holm-Bonferroni correction). Right, average nicotine consumption (mg/kg/d) in $\beta4^{-/-}$
858 and WT mice as a function of the concentration of nicotine in the bottle (Friedman test,
859 n = 35, df = 3, $p < 0.001$ and Mann-Whitney post-hoc test with Holm-Bonferroni
860 correction). $\beta4^{-/-}$ mice consumed more nicotine than WT mice (Mann-Whitney test). **B.**
861 Ternary diagram representing each WT and $\beta4^{-/-}$ individual for its side success rate
862 over its nicotine success rate. Small dots correspond to the habituation period (water
863 vs. water) and bigger dots to the condition with 200 µg/ml of nicotine in one bottle.
864 Inserts: pie charts illustrating the proportion of avoiders (light grey) and consumers
865 (dark grey) for each genotype at the end of the task. Note the absence of avoiders in
866 $\beta4^{-/-}$ mice. **C.** Average distance from each apex during the two-bottle choice task (0,
867 10, 50, 100 and 200 µg/ml of nicotine, paired Mann-Whitney test with Holm-Bonferroni
868 correction, p(Sacc 0-200) = 0.0002, p(Sacc 0-100) = 0.03; p(Nic 0-200) = 0.0002,
869 p(Sacc 0-100) = 0.03). **D.** Left, representative currents following a puff application of
870 nicotine (30 µM, 200 ms) on IPN neurons from naive WT and $\beta4^{-/-}$ mice, or from saline-
871 treated (orange) and nicotine-treated (dark orange) $\beta4^{-/-}$ mice. Right, average nicotine-
872 evoked currents recorded in IPN neurons from naïve WT (n = 32, -370 $\pm$ 61 pA) and
873 $\beta4^{-/-}$ (n = 27, -83 $\pm$ 13 pA) mice, and from $\beta4^{-/-}$ chronically treated with either saline
874 (Sal, n = 30, -72 $\pm$ 11 pA) or nicotine (Nic, n = 31, -123 $\pm$ 21 pA). $\beta4^{-/-}$ mice presented
875 a large decrease in nicotine-evoked currents (Mann-Whitney test, p = 4e-05). Nicotine
876 treatment did not alter nicotine-evoked currents in IPN neurons of $\beta4^{-/-}$ mice (Mann-
877 Whitney test, p = 0.15). **E.** Juxtacellular recordings nicotine-evoked responses in IPN
878 neurons in naïve WT and $\beta4^{-/-}$ mice. Top, representative example of the variation in
879 firing frequency of an IPN neuron, following repeated i.v. injections of nicotine at 7.5,
880 15 and 30 µg/kg, in WT and $\beta4^{-/-}$ mice. Bottom left, dose-dependent change in firing
881 rate from baseline following i.v. injections of nicotine ($p < 0.05$). All recorded neurons

882 were neurobiotin-labelled to confirm their location within the IPN. Bottom right, average
883 nicotine-evoked responses at 30 μg/kg of nicotine in IPN neurons from WT and $\beta4^{-/-}$
884 mice. Insert, average amplitude of the change in firing frequency from baseline after
885 an i.v. injection of saline and nicotine (30μg/kg), for IPN neurons from WT and $\beta4^{-/-}$
886 mice. Nicotine-induced responses were lower in $\beta4^{-/-}$ than in WT mice ($p < 0.001$, Mann
887 Whitney test). In all figure panels WT animals are depicted in grey and $\beta4^{-/-}$ mice in
888 yellow. *** $p < 0.001$, ** $p < 0.01$, * $p < 0.05$.
889

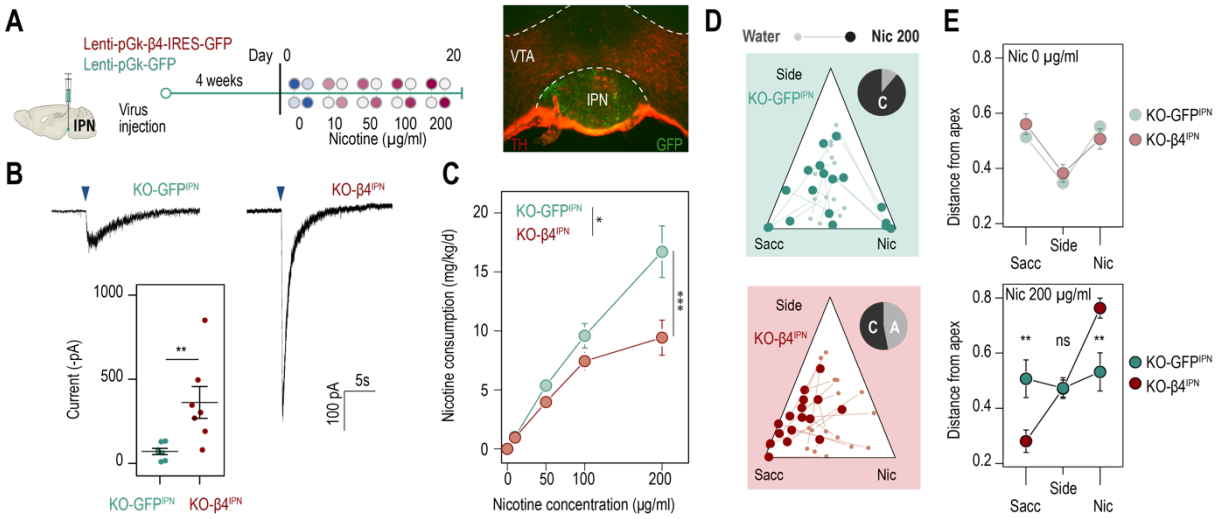

FIGURE 5

Figure 5: β4-containing nAChRs of the IPN are involved in the control of nicotine consumption and in spontaneous nicotine avoidance-like behavior in mice. A. Protocol: stereotaxic transduction of the β4 subunit together with GFP (or GFP alone in control mice) in the IPN of $\beta4^{-/-}$ mice, and subsequent two-bottle choice task. Right: coronal section highlighting proper viral transduction of lenti-pGK-β4-IRES-GFP in the IPN. **B.** Validation of the re-expression using patch-clamp electrophysiology recordings. Representative currents and average responses following a puff application of nicotine (30 µM, 200 ms) on IPN neurons from $\beta4^{-/-}$ mice transduced in the IPN with either lenti-pGK-β4-IRES-GFP (KO-$\beta4^{IPN}$, n = 7, -362 ± 95 pA) or lenti-pGK-GFP (KO-GFP^{IPN}, n = 7, -71 ± 18 pA; Mann-Whitney test, p = 0.004). **C.** Average nicotine consumption was lower in KO-$\beta4^{IPN}$ than in KO-GFP^{IPN} (two-way repeated measure; ANOVA: genotype x dose interaction, F[3, 99] = 6.3, ***p < 0.001; main effect of dose, F[3, 99] = 69.1 ***p < 0.001, effect of genotype, F[1, 33] = 6.637, *p = 0.015). **D.** Ternary diagram representing each $\beta4^{-/-}$ mouse, transduced with either β4 or GFP, and illustrating its side success rate over its nicotine success rate. Small dots correspond to the habituation period (water vs. water) and bigger dots to the condition with 200 µg/ml of nicotine in one bottle. Inserts: pie charts illustrating the proportion of

908 avoiders (light grey) and consumers (dark grey) for each condition at the end of the
909 task. **E.** Average distance from each apex during the two-bottle choice task at 0 and
910 200 µg/ml of nicotine, for KO-β4^{IPN} and KO-GFP^{IPN} mice. In all figure panels KO-β4^{IPN}
911 mice are depicted in red and KO-GFP^{IPN} mice (controls) in green. ($p_{Sacc} = 0.007$, $p_{Nic} =$
912 0.008, Mann-Whitney test with Holm-Bonferroni correction). *** $p < 0.001$, ** $p < 0.01$,
913 * $p < 0.05$.